

ProGraph: Temporally-alignable Probability Guided Graph Topological Modeling for 3D Human Reconstruction

Hongsheng Wang^{1,2}, Zehui Feng², Tong Xiao², Genfan Yang², Shengyu Zhang^{1,*},
Fei Wu¹, Feng Lin³

¹Zhejiang University, ²Zhejiang Lab ³Fuyao University of Science and Technology

Abstract

Current 3D human motion reconstruction methods from monocular videos rely on features within the current reconstruction window, leading to distortion and deformations in the human structure under local occlusions or blurriness in video frames. To estimate realistic 3D human mesh sequences based on incomplete features, we propose Temporally-alignable **Probability Guided Graph** Topological Modeling for 3D Human Reconstruction (ProGraph). For missing parts recovery, we exploit the explicit topological-aware probability distribution across the entire motion sequence. To restore the complete human, **Graph Topological Modeling** (GTM) learns the underlying topological structure, focusing on the relationships inherent in the individual parts. Next, to generate blurred motion parts, **Temporal-alignable Probability Distribution** (TPDist) utilizes the GTM to predict features based on distribution. This interactive mechanism facilitates motion consistency, allowing the restoration of human parts. Furthermore, **Hierarchical Human Loss** (HHLoss) constrains the probability distribution errors of inter-frame features during topological structure variation. Our Method achieves superior results than other SOTA methods in addressing occlusions and blurriness on 3DPW.

Introduction

3D human pose and shape reconstruction models find applications in various fields such as medical rehabilitation, game development, sports analysis, and clothing design (Lupi3n et al. 2024; Du et al. 2024; Yan et al. 2024). Scenes captured by monocular cameras often exhibit occlusion and depth blur due to motion. One of the significant technical challenges that arise in this context is accurately estimating the 3D human body mesh sequence based on incomplete human features in single-view scenarios.

3D human body video reconstruction aims to estimate the real 3D human body mesh, and its technical means can be roughly classified into regression-based reconstruction methods and probability distribution-based reconstruction methods. Regression methods focus primarily on frame prediction and lack cross-frame feature dependency modeling without exploiting long-term dependencies. To reconstruct a realistic 3D human body mesh under occlusion blurred segments, methods based on direct learning of spatial position

alignment of 3D human body geometrical structures for direct regression are employed (Cho, Youwang, and Oh 2022a; Goel et al. 2023). These methods can perceive the topological structure of the human body in the current frame. However, these methods make it difficult to predict the motion features of the same sequence over long distances between different frames. When the body moves, occluding, etc., features can be lost, resulting in inaccurate and distorted reconstruction (Sengupta, Budvytis, and Cipolla 2022). The other line of work Hierarchical autoregressively learns the rotation probability distribution of each joint according to the topological structure of the human kinematic tree. This is done by utilizing the distribution to improve the accuracy of joint reconstruction in occlusion-ambiguous scenarios (Sengupta, Budvytis, and Cipolla 2021). However, methods based on probability distribution also have limitations. Since the number of joints in the whole body is relatively sparse, it is difficult to represent the features of the joints in the whole body only through rotation probability distribution, which often leads to distortion and muscle stretching reconstruction results. Therefore, the introduction of topological relationships between vertices of the human body mesh is of vital importance in the probability distribution-based approach.

To align human body topology with 3D spatial features, we introduce a framework named ProGraph. This approach involves creating a probability distribution through human body mesh vertex topology-guided prediction. The framework aims to align features with the 3D geometry of the human body by constructing probability distributions based on feature spaces of the same topology in various frames within a sequence. Specifically, it focuses on capturing potential long-distance motion feature information and addressing missing features to guide the generation of human body topology.

ProGraph is organized into three modules. **Graph Topological Modelling** (GTM), uses the spatial dimension-based Graph Network module to explicitly learn the topological connections among the vertices of the body mesh and to transform the implicit topological connections within the human body into an explicit representation of a graph structure. This explicit connection ensures that in case of local node loss, it is possible to predict the missing nodes based on the graph structure. The first module can learn the topologi-

*Corresponding author: sy_zhang@zju.edu.cn

cal associations implicit in the human body from the current frame, but in order to maintain the stability of reconstruction results, the cross-frame feature dependencies implicit in the feature space are also needed, which can be expressed as a probability distribution over the 3D geometry of the human body. Therefore, we developed **Temporally-alignable Probability Distribution** (TPDist), which uses a time-guided latent diffusion module to align the probability distributions of the implied human 3D geometric structures between the adjacent frames in a time-guided manner. This approach is able to predict the probability distribution of the missing features with the aid of cross-frame dependency loss, in order to guide the regression of human topology and construct the coherence of the human mesh sequence. Meanwhile, to hierarchically calculate the error between the predicted results and the true values of different body parts, we proposed **Hierarchical Human Loss** (HHLoss), a progressive part-aware spatio-temporal loss to guide perception through the body. Finally, we use a non-parametric model reconstruction method to accurately restore the original human muscle movements.

Our contributions mainly lie in:

1. To the best knowledge, we make the first attempt to combine the temporally-alignable probability and graph Topology in 3D human pose and shape estimation. The proposed Temporally-alignable Probability Guided Graph Topological Modeling (ProGraph) merges the knowledge from probability distribution and human prior structures, improving our method’s accuracy.

2. In ProGraph, we carefully design Hierarchical Human Loss (HHLoss), for accurately calculating the progressive probability error of different body parts.

3. The experimental results reveal the effectiveness of ProGraph in 3D human mesh reconstruction, particularly its ability to excel in challenging scenarios involving occlusions and motion blur. Notably, our approach outperforms the state-of-the-art (SOTA) in video-based reconstruction on the 3DPW (von Marcard et al. 2018) dataset.

Related Work

There are two main categories of technical means for estimating 3D human pose and shape: regression-based reconstruction methods and probability distribution-based reconstruction methods. Spatial regression based methods (Cho, Youwang, and Oh 2022a; Lin et al. 2023) leverage transformer encoders to capture the non-local relationships between human joints and mesh vertices, which facilitates the reconstruction of three-dimensional human mesh from single images. Transformer-based human body reconstruction approaches can generally be categorized into two groups: parameterization methods that employ the SMPL model, and non-parametric methods that directly upsample regression grid vertices. Notably, parameterization approaches, such as SMPLify (Bogo et al. 2016) and Akash Sengupta *et al.* (Sengupta, Budvytis, and Cipolla 2022) have notably demonstrated success in estimating 3D body shape and pose from 2D joints. However, due to their reliance on strong structural priors, these methods may encounter difficulties

in cases of severe occlusion or ambiguity, potentially constraining the reconstruction outcomes within a predefined embedding space and hindering alignment with 2D information. In contrast, non-parametric methods offer direct regression of the body shape using forms such as voxels (Cohen and Li 2003; Zheng et al. 2019) or the three-dimensional positions of grid vertices (Moon and Lee 2020; Lin, Wang, and Liu 2021b), bypassing the need for parameter prediction. Non-parametric approaches are inherently flexible and often outperform model-based methods in accurately capturing the nuances of human muscle movement. Building on these advancements, our work employs non-parametric methods, achieving results that surpass current state-of-the-art (SOTA) outcomes (Zhou et al. 2023; Guo, Python, and Liu 2022) in various metrics.

Probability distribution-guided models, particularly those based on Markov chains (Song, Meng, and Ermon 2022; Ho, Jain, and Abbeel 2020), have demonstrated remarkable success in various computer vision applications, such as image generation (Nichol and Dhariwal 2021; Rombach et al. 2022; Dhariwal and Nichol 2021), super-resolution (Saharia et al. 2021; Ho et al. 2021), and video generation (Li et al. 2023c; Blattmann et al. 2023a,b). Liu *et al.* (Liu et al. 2019) introduced Constrained Spatial Smoothing (CSS) for spatial data reconstruction, which has been applied in various domains. Guo *et al.* (Guo, Python, and Liu 2022) extended regionalization algorithms to address spatial process heterogeneity, providing new insights into spatial data analysis. Diffusion models, capable of learning sample probability distributions, have been applied in innovative ways. For example, Gene Chou *et al.* (Li et al. 2023b) introduced DiffusionSDF for point cloud completion and reconstruction, predicting real point cloud distributions from sparse samples and achieving impressive results. The Flow method (Sengupta, Budvytis, and Cipolla 2023) models human body posture and shape by mapping data to a low-dimensional latent space for representation, generation, and transformation, showing promising predictive capabilities. Similar to our work, DiffMesh (Zheng et al. 2023a) generates accurate output mesh sequences by learning the probability distribution of human motion in both the forward and backward processes of the diffusion model. However, it may produce unreasonable mesh outputs in scenes with significant occlusion.

Our contribution, ProGraph, integrates human body topology guidance to enhance hierarchical perception of human joint structures within a frame, mitigating implausible reconstruction outcomes. Additionally, the use of probability distribution models enables our method to effectively track reconstructed characters in dynamic scenes, accurately infer missing structural details between successive frames, and reduce jitter in the reconstruction results.

Method

Overview

Our framework, illustrated in Figure 1 revolves around three key components: Temporally-aligned Probability Distribution (TPDist), Graph Topological Modeling (GTM), and Hi-

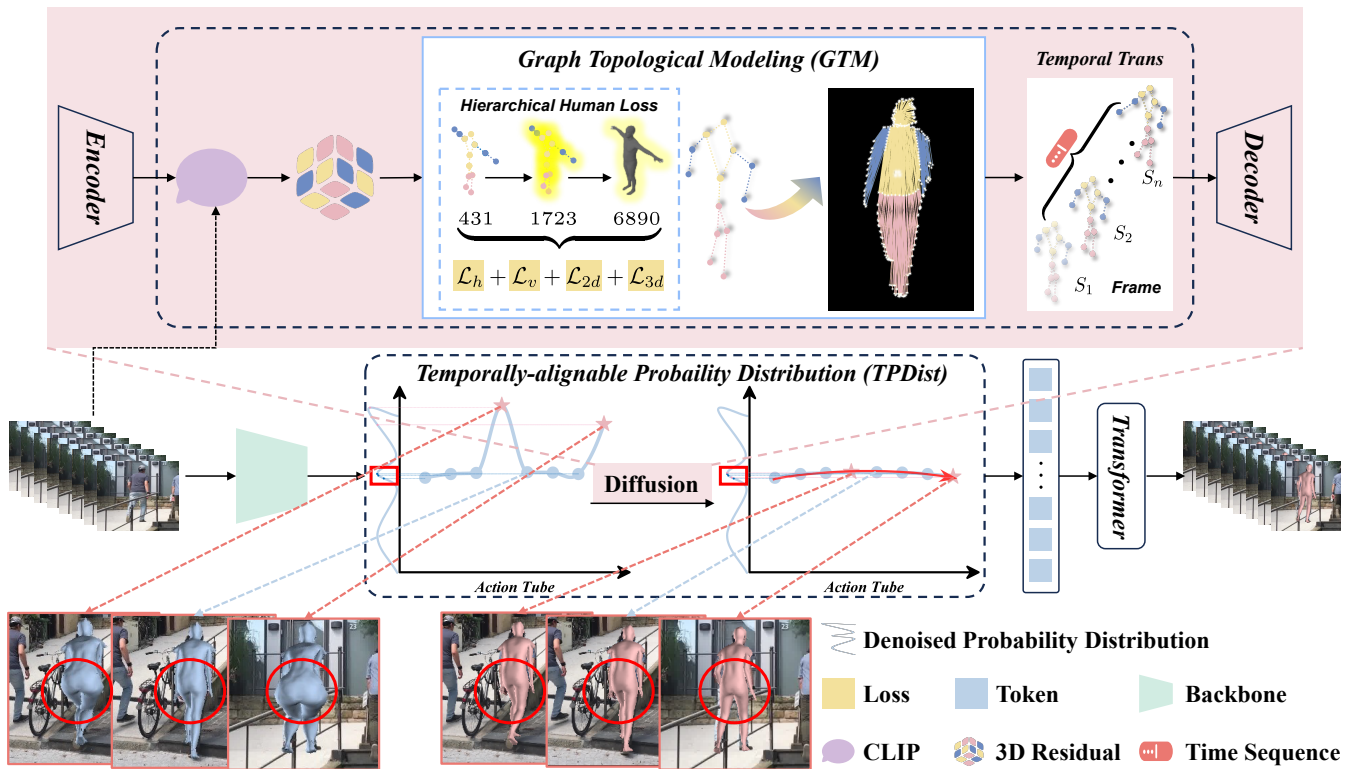


Figure 1: Overview framework. The ProGraph consists of three main components: Temporally-alignable Probability Distribution (TPDist), Graph Topological Modeling (GTM), and Hierarchical Human Loss (HHLoss). Given latent features extracted from the HRNet-W64 backbone, TPDist learns temporally consistent motion features. It leverages the probability distribution of the human body topology within the latent space, as guided by GTM. This enables TPDist to capture information about missing regions due to occlusions.

erarchical Human Loss (HHLoss). Given an RGB video as input, GTM progressively encodes the latent space for each frame, capturing the underlying human topological structure. TPDist then leverages GTM to learn the temporal evolution of feature probability distributions for each body part across the entire motion sequence. Subsequently, HHLoss hierarchically constrains the feature errors for each body part, ensuring their consistency. Hierarchically refers to the purpose of the HHLoss: unite errors generated during multi-hierarchical downsampling of GTMs. This synergistic interplay between GTM and TPDist enables accurate 3D body mesh generation, even in scenarios with occluded body parts. The following section details the specific considerations incorporated into our model.

Graph Topological Modeling (GTM)

Local occlusions within motion sequences frequently result in missing details within the feature space. Existing methods often struggle to recover fine details from monocular video inputs, leading to the potential loss of feature details due to localized occlusion (Xu, Fujita, and Matsumoto 2022). To address this limitation, we introduce Graph Topological Modeling (GTM). This module guides the model to exploit the inherent relationships within the human body’s topology. To effectively leverage the human body’s topological struc-

ture, GTM performs a dimensionality reduction. It downsamples the 6890 vertices in the SMPL model (Loper et al. 2015) to 431 vertices through linear projection. This focuses on the model’s representation of key aspects of the body structure. Subsequently, GTM transforms the implicit connections between these vertices into an explicit graph structure using an adjacency matrix. This process allows GTM to explicitly model the relationships between body parts, rather than relying solely on the individual vertex information. Figure 2 illustrates the mapping between the prior association information of the vertices and the resulting explicit graph structure.

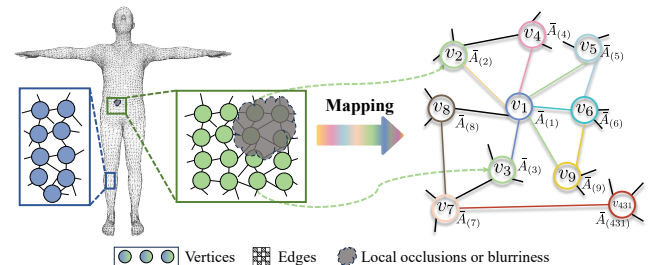


Figure 2: The mapping process between the prior association information of the vertices and the explicit graph structure.

Graph convolution is used to map the explicit graph information to the human body structure in the latent space. For the potential spatial dimension of the latent space ($C \times H \times W$), each frame of the sequence is a latent space containing the structural features of the target human body $Y = \{Y_1, Y_2, \dots, Y_n\}$, $Y \in \mathbb{R}^{n \times c}$, where C denotes the latent size, H and W represent the height and width of each image frame, and Y represents the vector of GraphConv module output, the process of graph convolution is shown in Equation 1:

$$Y' = \text{GraphConv}(\bar{A}_{\text{Smpl}}, Y; W_G) = \sigma(\bar{A}_{\text{Smpl}} Y W_G) \quad (1)$$

where, $\bar{A}_{\text{Smpl}} \in \mathbb{R}^{n \times n}$ is the adjacency matrix of the explicit graph structure, which contains prior information about human body parts and their associations guided by the SMPL model, W_G is the trainable parameter, and $\sigma(\cdot)$ is the activation function that imparts nonlinearity to the network.

Temporally-alignable Probability Distribution (TPDist)

While the (GTM) module enhances the model’s resilience against local feature errors, it can still occasionally produce jittering artifacts in the mesh vertices when faced with ambiguous input. To address this limitation, we introduce the Temporally-aligned Probability Distribution (TPDist) module. TPDist tackles the jittering phenomenon and recovers blurred body regions by learning the probability distribution of features for each body part across the entire motion sequence. This comprehensive understanding of feature distribution allows TPDist to predict missing or ambiguous information, leading to smoother and more robust mesh reconstructions.

TPDist introduces a Temporal Transformer layer after GTM. This layer defines the sequence-aware temporal backbone to align the human topology encoded by GTM frame-by-frame in a temporally consistent manner. Given a sequence data $x \in \mathbb{R}^{(BT) \times C \times H \times W}$, where BT is the batch size and time steps, C is the number of latent channels, H and W are the spatial potential dimensions. The TPDist process is shown as follows (Rogozhnikov 2021):

$$x_t = \sqrt{1 - \alpha_t} \cdot \varepsilon_t + \sqrt{\alpha_t} \cdot x_{t-1} \quad (2)$$

$$x_t = \text{CrossAttention}(\gamma_A, x_t) \quad (3)$$

where ε is the Gaussian noise, x_t is the input to the hidden space at moment t of the noise addition process, α_t is a value between [0.0, 1.0] as a coefficient, and γ_A is a latent feature (Wang, Xing, and Liu 2021) obtained from the video stream to gradually enhance the action-semantic information of the human body in the process of noise addition.

$$x \leftarrow \text{rearrange}(x_t, (BT) C H W \rightarrow BT C H W)$$

$$x = 3DConv(x; W_H) = \sigma(x W_H) \quad (4)$$

$$x = \text{GraphConv}(x; \bar{A}_{\text{smpl}}) \quad (5)$$

where W_H is a trainable parameter. It interprets the full noise, x_t as a batch of independent data with human body topological information. The module encodes it frame-by-frame using GTM to enhance topological information within each frame.

$$x \leftarrow \text{rearrange}(x, B T C H W \rightarrow (B H W) T C)$$

$$\delta = \text{SelfAttention}(x) \quad (6)$$

To extract temporally consistent features, we synchronize the temporal information with the frame-level topological structure. We achieve this by reorganizing the temporal dimensions to decouple the latent features. This ensures that each resulting structure incorporates information from the entire time series. Subsequently, a Temporal Transformer model is applied along the temporal dimension t to capture the dependencies δ among identical topological structures across various time steps.

$$x_t \leftarrow \text{rearrange}(x, (B H W) T C \rightarrow (B T) C H W)$$

$$z_t = \text{CrossAttention}(\delta, x_t) \quad (7)$$

$$z_{t-1} = \frac{1}{\sqrt{\alpha_t}} \left(z_t - \frac{1 - \alpha_t}{\sqrt{1 - \alpha_t}} \varepsilon(z_t, t) \right) + \frac{\sqrt{1 - \alpha_t} \sqrt{1 - \alpha_{t-1}}}{\sqrt{1 - \alpha_t}} I \quad (8)$$

Following the processing by GTM and the Temporal Transformer layer, the data is reshaped back into video dimensions, where I represents a standard Gaussian distribution. Here, the captured dependencies δ_t act as the conditional space, guiding the decoding process within the latent space. This approach enhances the propagation of structural information throughout the sequence. Finally, DDPM (Ho, Jain, and Abbeel 2020) process is employed to yield a probability distribution of features that aligns with the 3D geometric structure of the human body.

To achieve a comprehensive understanding of the human body’s structure throughout motion, ProGraph employs the GTM and Temporal Transformer layer iteratively. This two-pass approach constructs a richer graph structure with broader vertex associations, leading to a more complete mapping within the latent space. Consequently, ProGraph is empowered to learn the targeted topological sequences in a spatio-temporally consistent manner. This enhanced learning process translates to improved model accuracy and stability in restoring occluded or blurred body parts. ProGraph achieves this by resampling features from the target probability distribution with the highest confidence scores within the sequences. Figure 3 illustrates the underlying processes of our network.

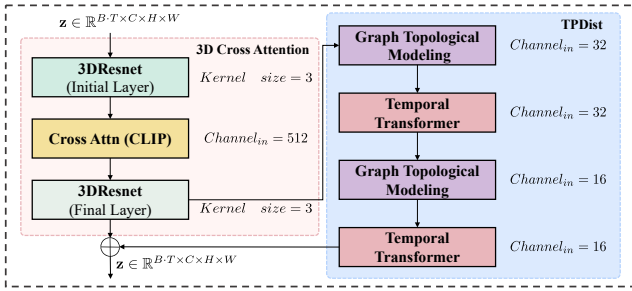


Figure 3: The ProGraph network architecture integrates a 3D ResNet with CLIP for cross-attention. It also employs a dual-pathway approach, combining Graph Topological Reconstruction and Temporal 3D Transformers. This approach facilitates the alignment of the topological and geometric structures of human body meshes across a video sequence.

Hierarchical Human Loss

In this work, we introduce TPDist, a method that leverages GTM to learn the probability distribution of human body topology. To guarantee consistent topological representation, we propose a novel hierarchical manual guidance approach for the semantic segmentation of 6890 vertices. This approach involves learning the probability distribution of corresponding vertex features at various levels within a region. Subsequently, the error of the vertices is adaptively constrained in a hierarchical manner at each upsampling step.

Prior to the transformer module, our approach employs FastMetro (Cho, Youwang, and Oh 2022a) to upsample the spatio-temporally aligned human body topology, which incorporates semantic information by subdividing nodes based on body part labels at each step. To avoid spatial redundancy, the sequences are then sampled back to the original resolution (6,890 SMPL mesh vertices) using linear projection. To capture the hierarchical structure and guide the alignment process, we employ softmax pooling to obtain the sequence probability distribution of body parts. Finally, cross-entropy is used to evaluate the difference between the predicted and true distributions for hierarchical topological association alignment.

$$\begin{aligned}
 y &= \text{logsoftmax}(x_{ij}) = \log\left(\frac{e^{x_{ij}-c}}{\sum_k e^{x_{ij}-c}}\right) \\
 &= (x_{ij} - c) - \log\left(\sum_k e^{x_{ij}-c}\right)
 \end{aligned} \quad (9)$$

$$\mathcal{L}_p(y_{\text{pred}}, y_{\text{true}}) = y_{\text{true}} \cdot (\log y_{\text{true}} - \log y_{\text{pred}}) \quad (10)$$

where x is the input tensor ($B, N, 3$). B is the size of the batch data, N is the size of the indexed interval of vertices with well-categorized labels. And y denotes the probability distribution. i is the index of the batch, j is the index of the lattice vertices. We operate along the dimensionality N , with $c = \max(x_{ij})$, c to constrain the tensor x_{ij} from exceeding to denote the indexed range of the current lattice vertices.

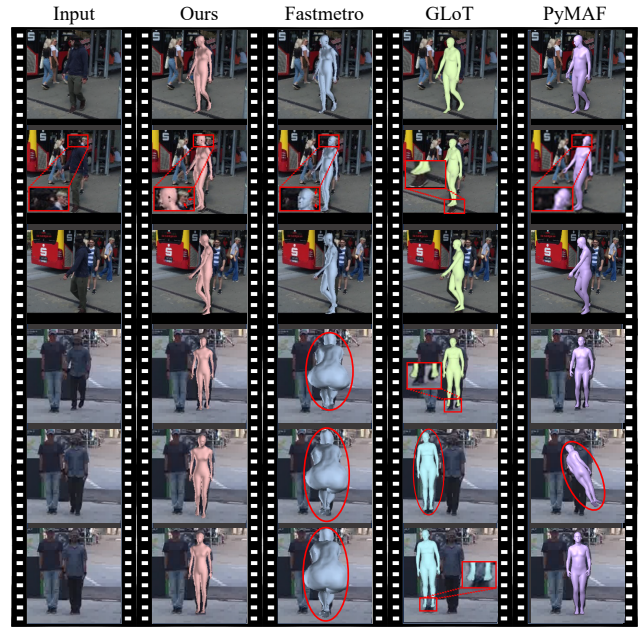


Figure 4: An analysis and comparison of inter-frame prediction results. The original image is presented on the far left, with the outputs of our model, Fastmetro, GLoT, and PyMAF displayed sequentially to the right.

Human body perception varies across different parts. To account for this, we propose a method that dynamically inherits weights for each body part from the GTM, which reflect the influence of each part on the overall body representation. The weight for a specific part λ is derived from its variance within the GTM, allowing for adaptive tuning of the local influence on the entire body during training.

Inspired by the detailed vertex classifications of the SMPL model, our method incorporates a fine-grained classification denoted as \mathcal{L} and progressively aligns the loss functions associated with the probability distributions for each body part during the upsampling process. This classification scheme utilizes indexed ranges for each label, denoted as (s_l, e_l) , where l iterates over the total number of labels m .

$$\mathcal{L}_{Human} = \sum_{p=1}^n \lambda_p \mathcal{L}_p \cdot \left(\bigvee_{l=1}^m (p \geq s_l \wedge p \leq e_l) \right) \quad (11)$$

Experiments

Datasets and metrics

We leverage publicly available datasets for training our model, including Human3.6M (Han et al. 2017) and 3DPW (von Marcard et al. 2018). The 3DPW dataset is used for both training and fine-tuning the model. We evaluate the model's performance on the 3DPW test set. For Human3.6M evaluations, we adhere to the P2 protocol setting. Consistent with prior works (Kanazawa et al. 2019; Kocabas, Athanasiou, and Black 2020; Wei et al. 2022), we employ three

Table 1: This table analyzes the influence of the Temporally-Aligned Probability Distribution (TPDist) module and loss functions on 3D human mesh reconstruction performance across the 3DPW and Human3.6M datasets. We evaluate performance using MPVE, MPJPE, and PA-MPJPE metrics. Lower values in these metrics consistently indicate higher accuracy in reconstructing the 3D human mesh.

TPDist	Loss	3DPW			Human3.6M	
		MPVE↓	MPJPE↓	PA-MPJPE↓	MPJPE↓	PA-MPJPE↓
×	×	85.5	73.9	44.9	51.9	33.8
✓	×	82.35	72.79	44.12	49.9	33.7
×	✓	81.93	72.81	44.03	49.5	33.2
✓	✓	81.89	72.72	43.82	49.1	33.1

Table 2: Comparison of frame-based methods and video-based methods on 3DPW and Human3.6M datasets.

Method	Output-type	3DPW			Human3.6M	
		MPVPE↓	MPJPE↓	PA-MPJPE↓	MPJPE↓	PA-MPJPE↓
Frame based						
Graphormer(Lin, Wang, and Liu 2021b)	vertices	87.7	74.7	45.6	51.2	34.5
METRO (Lin, Wang, and Liu 2021a)	vertices	88.2	77.1	47.9	54.0	36.7
Hybrik-X (Li et al. 2023a)	parameters	94.5	80.0	48.8	-	-
Pymaf-X (Zhang et al. 2023)	parameters	110.1	92.8	58.9	57.7	40.5
Potter (Zheng et al. 2023b)	parameters	87.4	75.0	44.8	56.5	35.1
Fastmetro (Cho, Youwang, and Oh 2022b)	vertices	84.1	73.5	44.6	52.2	33.7
PointHMR (Kim et al. 2023)	vertices	85.5	73.9	44.9	48.3	32.9
Video based						
HMMR (Kanazawa et al. 2019)	parameters	139.3	116.5	72.6	-	56.9
VIBE (Kocabas, Athanasiou, and Black 2020)	parameters	99.1	82.9	51.9	65.6	41.4
TCMR (Choi et al. 2021)	parameters	111.3	95.0	55.8	62.3	41.1
MAED (Wan et al. 2021)	parameters	92.6	79.1	45.7	56.4	38.7
MPS-Net (Wei et al. 2022)	parameters	109.6	91.6	54.0	69.4	47.4
GLoT (Shen et al. 2023)	parameters	96.3	80.7	50.6	67.0	46.3
4DHumans (Goel et al. 2023)	parameters	82.2	70.0	44.5	44.8	33.6
Ours	vertices	82.12	72.72	43.82	49.1	33.1

intra-frame metrics for evaluation: MPJPE, MPJPE, and PA-MPJPE.

Ablation Study

Temporally-alignable Probability Distribution (TPDist) is implemented on the basis of Graph Topological Modeling (GTM), in this section, we will perform two sets of ablation studies, on the 3DPW and Human3.6M datasets to validate the effectiveness of the key modules proposed in our approach. All ablation methods are trained and tested on both datasets, which are widely used benchmarks for 3D human pose and shape reconstruction.

Efficacy of TPDist. TPDist learns the probability distribution of each part, guiding the occlusion and blurring of certain parts for more accurate perception. This allows for efficient extraction of spatial features, thereby improving the quality of 3D human generation. To verify the effectiveness of the module, a set of ablation experiments was conducted. Table 1 compares the performance of our model with and without TPDist during training. The results show that the TPDist reduces the MPJPE and PA-MPJPE metrics by 2.4mm and 0.6mm respectively on the Human3.6M dataset, and by 3.57mm for MPVPE, MPJPE, and PA-MPJPE metrics on the 3DPW dataset. These reductions indicate that TPDist effectively guides the probability distribution between the predicted results and ground truth, leading to more accurate human mesh reconstruction.

Benefit from HHLoss. We compare the method using HHLoss with the baseline. As shown in Table 1, the HHLoss method achieves significant improvements on both the Human3.6M and 3DPW datasets. On Human3.6M, it reduces MPJPE by 1.93mm and PA-MPJPE by 0.1mm. Even more notably, on 3DPW, it reduces MPVPE, MPJPE, and PA-MPJPE by 3.15mm, 1.11mm, and 0.78mm, respectively. These results demonstrate the effectiveness of the HHLoss module’s ability to adaptively learn probability distributions at the time level, leading to more accurate 3D human pose estimation.

Validating the interaction between TPDist and HHLoss.

Table 1 showcases the significant improvements achieved by combining TPDist and HHLoss compared to a baseline model. On the Human3.6M dataset, our method reduces MPJPE by 2.8mm and PA-MPJPE by 0.7mm. Even more impressive are the results on 3DPW, where MPVPE, MPJPE, and PA-MPJPE are reduced by 3.15mm, 1.11mm, and 0.78mm, respectively. These reductions **surpass the improvements achievable with each module individually**, demonstrating the synergistic effect of TPDist and HHLoss in enhancing 3D human pose estimation accuracy.

Comparative Study

Qualitative Analysis. Compared with the existing methods, ProGraph effectively tackles the challenge of human

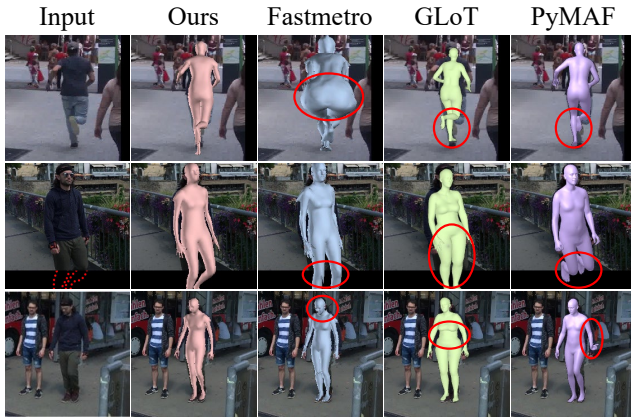


Figure 5: This figure conducts analysis and comparison of intra-frame prediction results, showcasing the capability to handle complex scenes, such as walking people. The original image is displayed on the far left, followed to the right by the outputs of our model, Fastmetro, GLoT, and PyMAF, respectively.

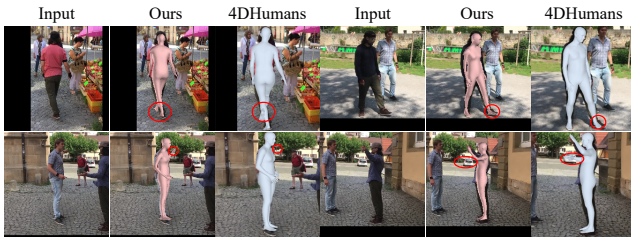


Figure 6: The comparison of our framework and 4DHumans. The red circles around the feet areas emphasize the superior precision of our model’s pose estimation, particularly in challenging scenarios with intricate backgrounds or complex poses.

body distortion caused by missing or unclear parts of the human body. The following shows the comparison effect:

Figure 4 illustrates the comparative effects of reconstructing different human motion sequences in two scenarios with missing or unclear body parts. The first three rows represent the first motion sequence, while the last three rows represent the second sequence. In the first motion sequence (top rows), both FastPose and PyMAF suffer from severe head distortions. This is likely because the input image has a blurry head region. These methods mistakenly use features from nearby, non-target people to reconstruct the head, leading to inaccuracies. Similarly to the second motion sequence, GLoT fails to accurately reconstruct the foot position due to ambiguity in the target foot region of the input image. Our ProGraph framework addresses these challenges by learning the probability distribution of each body part across the entire motion sequence. This learning leverages the explicit body topology information extracted from each 2D frame. Even if a particular body part is unclear or blurred in a single frame, ProGraph can still reconstruct it accurately by sampling from the real probability distributions learned from

other frames in the sequence.

To evaluate our method’s ability to handle incomplete or unclear body parts, we conducted comparative experiments across three scenarios. Figure 5 showcases the reconstruction results, comparing our approach with existing methods. The results demonstrate that FastMetro, GLoT, and PyMAF struggle to recover accurate human body mesh information for occluded or missing body parts. In contrast, our proposed GTM module explicitly captures the body’s topology through a graph structure. This allows GTM to learn the intrinsic correlations between different body mesh vertices. Consequently, even in scenarios with occlusions, blurry images, or missing local features, GTM can leverage these correlations to predict the missing information and achieve more accurate reconstructions.

To visually demonstrate ProGraph’s effectiveness, we compared it with 4DHumans on the 3DPW dataset Figure 6. In the first line, the reconstruction result of 4DHumans show incorrect estimation of the legs and feet. Similarly, in the second line of the scene, the torso and upper arm are obscured, leading to incorrect inferences by 4DHumans regarding the arm position.

Quantitative Analysis.

(i) **ProGraph Outperforms Video-based Methods.** We compare ProGraph with video-based methods on the 3DPW dataset. As shown in Table 2, ProGraph achieves superior performance on most evaluation metrics. Notably, compared to 4DHumans, our method reduces MPVPE and PA-MPJPE by 3.1mm and 0.6mm, respectively. These results establish ProGraph as a new state-of-the-art method for accurate human mesh reconstruction.

(ii) **ProGraph Outperforms Frame-based Methods.** To validate the effectiveness of our framework in 3D human pose and shape reconstruction, we compare ProGraph with previous frame-based methods on the 3DPW dataset using the MPVPE, MPJPE, and PA-MPJPE metrics. As shown in Table 2, we outperform the existing methods on all metrics. For example, ProGraph reduces MPVPE by 3.38 mm, MPJPE by 1.18 mm, and PA-MPJPE by 1.08 mm compared with PointHMR on 3DPW. The effectiveness of our method is demonstrated by the significant advantages of these metrics. Experimental results show that we still have the superiority even on frame-based methods.

Visualization Results

Visualization of TPDist. As Figure 7 shows, it visualizes the probability distribution of human body parts during the prediction process. The experimental results demonstrate that our method can leverage TPDist to achieve accurate reconstructions, even in complex scenes with occlusions or blurred body parts.

Results of wild images. Figure 8 shows ProGraph’s prediction results for obscured wild images. For wild pictures of complex scenes, ProGraph can effectively predict the probability distribution of human body parts to generate highly realistic human pose and shape estimations.



Figure 7: The reconstruction results and probability distribution of human body parts during the prediction process.



Figure 8: Human body reconstructions by our method. It enables accurate 3D human body reconstruction from videos, even with incomplete parts and occlusions, demonstrating exceptional robustness and high fidelity in 3D pose and shape reconstruction.

Conclusion

This work introduces ProGraph, a novel framework for reconstructing 3D human body mesh from monocular videos. ProGraph addresses the challenges of occlusion and blurriness by constructing probability distributions for human body topology across video frames. This significantly improves 3D human pose regression accuracy. Our framework outperforms state-of-the-art (SOTA) methods on 3DPW and Human3.6M, achieving superior reconstructions under challenging conditions. ProGraph’s robustness paves the way for various applications requiring accurate 3D pose estimation in unconstrained environments.

References

Blattmann, A.; Dockhorn, T.; Kulal, S.; Mendelevitch, D.; Kilian, M.; Lorenz, D.; Levi, Y.; English, Z.; Voleti, V.; Letts, A.; Jampani, V.; and Rombach, R. 2023a. Stable Video Diffusion: Scaling Latent Video Diffusion Models to Large Datasets. *arXiv:2311.15127*.

Blattmann, A.; Rombach, R.; Ling, H.; Dockhorn, T.; Kim, S. W.; Fidler, S.; and Kreis, K. 2023b. Align your Latents: High-Resolution Video Synthesis with Latent Diffusion Models. *arXiv:2304.08818*.

Bogo, F.; Kanazawa, A.; Lassner, C.; Gehler, P.; Romero, J.; and Black, M. J. 2016. Keep it SMPL: Automatic Estimation of 3D Human Pose and Shape from a Single Image. *arXiv:1607.08128*.

Cho, J.; Youwang, K.; and Oh, T.-H. 2022a. Cross-Attention of Disentangled Modalities for 3D Human Mesh Recovery with Transformers. In *European Conference on Computer Vision (ECCV)*.

Cho, J.; Youwang, K.; and Oh, T.-H. 2022b. Cross-Attention of Disentangled Modalities for 3D Human Mesh Recovery with Transformers. *arXiv preprint arXiv:2207.13820*.

Choi, H.; Moon, G.; Chang, J. Y.; and Lee, K. M. 2021. Beyond static features for temporally consistent 3d human pose and shape from a video. In *Proceedings of the IEEE/CVF conference on computer vision and pattern recognition, 1964–1973*.

Cohen, I.; and Li, H. 2003. Inference of human postures by classification of 3D human body shape. In *2003 IEEE International SOI Conference. Proceedings (Cat. No.03CH37443)*, 74–81.

Dhariwal, P.; and Nichol, A. 2021. Diffusion Models Beat GANs on Image Synthesis. *arXiv:2105.05233*.

Du, S.; Yuan, Z.; Lai, P.; and Ikenaga, T. 2024. Joy-Pose: Jointly learning evolutionary data augmentation and anatomy-aware global–local representation for 3D human pose estimation. *Pattern Recognition*, 147: 110116.

Goel, S.; Pavlakos, G.; Rajasegaran, J.; Kanazawa*, A.; and Malik*, J. 2023. Humans in 4D: Reconstructing and Tracking Humans with Transformers. In *International Conference on Computer Vision (ICCV)*.

Guo, H.; Python, A.; and Liu, Y. 2022. Extending regionalization algorithms to explore spatial process heterogeneity. *arXiv preprint arXiv:2206.09429*.

Han, F.; Reily, B.; Hoff, W.; and Zhang, H. 2017. Space-time representation of people based on 3D skeletal data: A review. *Computer Vision and Image Understanding*, 158: 85–105.

Ho, J.; Jain, A.; and Abbeel, P. 2020. Denoising Diffusion Probabilistic Models. *arXiv:2006.11239*.

Ho, J.; Saharia, C.; Chan, W.; Fleet, D. J.; Norouzi, M.; and Salimans, T. 2021. Cascaded Diffusion Models for High Fidelity Image Generation. *arXiv:2106.15282*.

Kanazawa, A.; Zhang, J. Y.; Felsen, P.; and Malik, J. 2019. Learning 3D Human Dynamics from Video. *arXiv:1812.01601*.

Kim, J.; Gwon, M.-G.; Park, H.; Kwon, H.; Um, G.-M.; and Kim, W. 2023. Sampling is Matter: Point-guided 3D Human Mesh Reconstruction. In *Proceedings of the IEEE/CVF Conference on Computer Vision and Pattern Recognition*, 12880–12889.

Kocabas, M.; Athanasiou, N.; and Black, M. J. 2020. VIBE: Video Inference for Human Body Pose and Shape Estimation. *arXiv:1912.05656*.

Li, J.; Bian, S.; Xu, C.; Chen, Z.; Yang, L.; and Lu, C. 2023a. HybriK-X: Hybrid Analytical-Neural Inverse Kinematics for Whole-body Mesh Recovery. *arXiv preprint arXiv:2304.05690*.

Li, M.; Duan, Y.; Zhou, J.; and Lu, J. 2023b. Diffusion-SDF: Text-to-Shape via Voxelized Diffusion. *arXiv:2212.03293*.

- Li, P.; Liu, Z.; Chen, K.; Hong, L.; Zhuge, Y.; Yeung, D.-Y.; Lu, H.; and Jia, X. 2023c. TrackDiffusion: Multi-object Tracking Data Generation via Diffusion Models. arXiv:2312.00651.
- Lin, J.; Zeng, A.; Wang, H.; Zhang, L.; and Li, Y. 2023. One-Stage 3D Whole-Body Mesh Recovery with Component Aware Transformer. *CVPR*.
- Lin, K.; Wang, L.; and Liu, Z. 2021a. End-to-End Human Pose and Mesh Reconstruction with Transformers. In *2021 IEEE/CVF Conference on Computer Vision and Pattern Recognition (CVPR)*, 1954–1963.
- Lin, K.; Wang, L.; and Liu, Z. 2021b. Mesh Graphormer. arXiv:2104.00272.
- Liu, B.; Mavrin, B.; Kong, L.; and Niu, D. 2019. Spatial Data Reconstruction via ADMM and Spatial Spline Regression. *Applied Sciences*, 9(9): 1733.
- Loper, M.; Mahmood, N.; Romero, J.; Pons-Moll, G.; and Black, M. J. 2015. SMPL: A Skinned Multi-Person Linear Model. *Acm Transactions on Graphics*, 34(6cd): 248.
- Lupi3n, M.; Polo-Rodr3guez, A.; Medina-Quero, J.; Sanjuan, J. F.; and Ortigosa, P. M. 2024. 3D Human Pose Estimation from multi-view thermal vision sensors. *Information Fusion*, 104: 102154.
- Moon, G.; and Lee, K. M. 2020. I2L-MeshNet: Image-to-Lixel Prediction Network for Accurate 3D Human Pose and Mesh Estimation from a Single RGB Image. arXiv:2008.03713.
- Nichol, A.; and Dhariwal, P. 2021. Improved Denoising Diffusion Probabilistic Models. arXiv:2102.09672.
- Rogozhnikov, A. 2021. Einops: Clear and reliable tensor manipulations with einstein-like notation.
- Rombach, R.; Blattmann, A.; Lorenz, D.; Esser, P.; and Ommer, B. 2022. High-Resolution Image Synthesis with Latent Diffusion Models. arXiv:2112.10752.
- Saharia, C.; Ho, J.; Chan, W.; Salimans, T.; Fleet, D. J.; and Norouzi, M. 2021. Image Super-Resolution via Iterative Refinement. arXiv:2104.07636.
- Sengupta, A.; Budvytis, I.; and Cipolla, R. 2021. Hierarchical kinematic probability distributions for 3D human shape and pose estimation from images in the wild. In *Proceedings of the IEEE/CVF international conference on computer vision*, 11219–11229.
- Sengupta, A.; Budvytis, I.; and Cipolla, R. 2022. Hierarchical Kinematic Probability Distributions for 3D Human Shape and Pose Estimation from Images in the Wild. arXiv:2110.00990.
- Sengupta, A.; Budvytis, I.; and Cipolla, R. 2023. HuMan-iFlow: Ancestor-Conditioned Normalising Flows on SO(3) Manifolds for Human Pose and Shape Distribution Estimation. arXiv:2305.06968.
- Shen, X.; Yang, Z.; Wang, X.; Ma, J.; Zhou, C.; and Yang, Y. 2023. Global-to-Local Modeling for Video-based 3D Human Pose and Shape Estimation. In *Proceedings of the IEEE/CVF Conference on Computer Vision and Pattern Recognition*, 8887–8896.
- Song, J.; Meng, C.; and Ermon, S. 2022. Denoising Diffusion Implicit Models. arXiv:2010.02502.
- von Marcard, T.; Henschel, R.; Black, M.; Rosenhahn, B.; and Pons-Moll, G. 2018. Recovering Accurate 3D Human Pose in The Wild Using IMUs and a Moving Camera. In *European Conference on Computer Vision (ECCV)*.
- Wan, Z.; Li, Z.; Tian, M.; Liu, J.; Yi, S.; and Li, H. 2021. Encoder-decoder with multi-level attention for 3d human shape and pose estimation. In *Proceedings of the IEEE/CVF International Conference on Computer Vision*, 13033–13042.
- Wang, M.; Xing, J.; and Liu, Y. 2021. ActionCLIP: A New Paradigm for Video Action Recognition. arXiv:2109.08472.
- Wei, W.-L.; Lin, J.-C.; Liu, T.-L.; and Liao, H.-Y. M. 2022. Capturing Humans in Motion: Temporal-Attentive 3D Human Pose and Shape Estimation from Monocular Video. arXiv:2203.08534.
- Xu, T.; Fujita, Y.; and Matsumoto, E. 2022. Surface-Aligned Neural Radiance Fields for Controllable 3D Human Synthesis.
- Yan, R.; Yin, Q.; Zhang, X.; Zhang, Q.; Zhang, G.; and Ma, S. 2024. Pose-Driven Compression for Dynamic 3D Human via Human Prior Models. *IEEE Transactions on Pattern Analysis and Machine Intelligence*, 1–15.
- Zhang, H.; Tian, Y.; Zhang, Y.; Li, M.; An, L.; Sun, Z.; and Liu, Y. 2023. Pymaf-x: Towards well-aligned full-body model regression from monocular images. *IEEE Transactions on Pattern Analysis and Machine Intelligence*.
- Zheng, C.; Liu, X.; Liu, M.; Wu, T.; Qi, G.-J.; and Chen, C. 2023a. DiffMesh: A Motion-aware Diffusion-like Framework for Human Mesh Recovery from Videos. *arXiv preprint arXiv:2303.13397*.
- Zheng, C.; Liu, X.; Qi, G.-J.; and Chen, C. 2023b. POTTER: Pooling Attention Transformer for Efficient Human Mesh Recovery. In *Proceedings of the IEEE/CVF Conference on Computer Vision and Pattern Recognition*, 1611–1620.
- Zheng, Z.; Yu, T.; Wei, Y.; Dai, Q.; and Liu, Y. 2019. DeepHuman: 3D Human Reconstruction From a Single Image. In *2019 IEEE/CVF International Conference on Computer Vision (ICCV)*, 7738–7748.
- Zhou, B.; Meng, D.; Franco, J.-S.; and Boyer, E. 2023. Human Body Shape Completion with Implicit Shape and Flow Learning. *Applied Sciences*, 9(9): 1733.